Speed-Adaptive Full-Order Observer Revisited: Closed-Form Design for Induction Motor Drives

Lauri Tiitinen
Aalto University
Espoo, Finland
lauri.tiitinen@aalto.fi

Marko Hinkkanen
Aalto University
Espoo, Finland
marko.hinkkanen@aalto.fi

Lennart Harnefors
ABB Corporate Research
Västerås, Sweden
lennart.harnefors@se.abb.com

***Abstract*—This paper deals with speed-adaptive full-order observer design for sensorless induction motor drives. The conventional full-order observer has been extensively investigated in the literature. Despite these efforts, the observer and its speed-adaptation mechanism are still not fully understood, and the tuning of the observer is often heuristic. Contrary to its reduced-order variant, direct pole-placement design has not been available for the full-order observer. This paper revisits the full-order observer and presents a new closed-form observer design, where the observer poles can be directly placed with simple design parameters.**

***Index Terms*—Estimation, induction machine, observer, sensorless, stability.**

I. Introduction

In sensorless induction machine drives, the control performance highly depends on the quality of the state estimates and thus on the design of the used observer. If the observer is well-designed, its dynamics can be tuned according to the desired control bandwidths and the noise characteristics of the drive system. This approach can be used implementing a reduced-order observer, since explicit pole-placement design is available for it [1].

The reduced-order observer estimates the rotor-flux linkage and the speed of the rotor. However, estimating also the stator current might be preferable, if good quality current measurement is not available. For this purpose, a full-order observer could be used. Although the full-order observer has been extensively investigated in the literature, explicit placement of the observer poles has not yet been available.

The full-order observer is a nonlinear observer, which uses a speed-adaptation loop to dynamically adapt the system matrix of the electrical quantities. The stability of conventional full-order observer designs were originally asserted with theories from nonlinear control theory [2], [3]. However, these analyses were made with incorrect assumptions, such as neglecting the flux estimation error, and the complete stability was not guaranteed [4], [5]. The stability issues of these pioneering works have been later considered with various observer gain proposals. The work in [6] proposes a completely stable framework for the observer gains with three free design parameters. The low-speed operation of this framework is improved in [7] with alternative gain-scheduling design for the free design parameters. Nevertheless, the link between the design parameters and the observer poles still remained unclear, and the tuning of the speed adaptation loop was not fully understood.

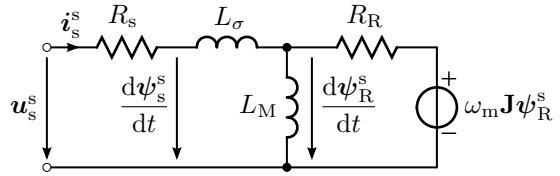

Fig. 1. Equivalent circuit of the induction motor in stator coordinates.

This paper proposes a new observer design for the full-order observer, which decouples the flux-estimation dynamics from the speed estimation. This decoupling is facilitated by the use of a non skew-symmetric gain matrix. It is shown by means of small-signal linearization that this design leads to a simple closed-form observer characteristic polynomial with complete stability, i.e. its local stability is guaranteed in the whole feasible operation region.

II. Motor Model

The induction motor is modeled using the standard inverse-Γ model [8], whose equivalent circuit is shown in Fig. 1. The stator current is represented by a column vector $\boldsymbol{i}_\mathrm{s} = [i_\mathrm{sd}, i_\mathrm{sq}]^\mathrm{T}$, where i_sd and i_sq are the d- and q-axis components, respectively, and the superscript T marks the transpose. Other vector quantities are represented similarly. The electrical rotor speed is denoted by ω_m. Furthermore, the identity matrix $\mathbf{I} = \left[\begin{smallmatrix}1 & 0\\ 0 & 1\end{smallmatrix}\right]$, the orthogonal rotation matrix $\mathbf{J} = \left[\begin{smallmatrix}0 & -1\\ 1 & 0\end{smallmatrix}\right]$, and the zero matrix $\mathbf{0} = \left[\begin{smallmatrix}0 & 0\\ 0 & 0\end{smallmatrix}\right]$ are used in the following equations.

The stator flux linkage $\boldsymbol{\psi}_\mathrm{s}$ and the stator current $\boldsymbol{i}_\mathrm{s}$ are used as the state variables. This selection is motivated by simplified gain matrices for the proposed full-order observer design. In a coordinate system rotating at the angular speed ω_s, the state equations are [9]

$$\frac{\mathrm{d}\boldsymbol{\psi}_\mathrm{s}}{\mathrm{d}t} = -\omega_\mathrm{s}\mathbf{J}\boldsymbol{\psi}_\mathrm{s} - R_\mathrm{s}\boldsymbol{i}_\mathrm{s} + \boldsymbol{u}_\mathrm{s} \tag{1a}$$

$$L_\sigma\frac{\mathrm{d}\boldsymbol{i}_\mathrm{s}}{\mathrm{d}t} = (\alpha\mathbf{I} - \omega_\mathrm{m}\mathbf{J})\boldsymbol{\psi}_\mathrm{s} - L_\sigma\left(\beta\mathbf{I} + \omega_\mathrm{r}\mathbf{J}\right)\boldsymbol{i}_\mathrm{s} + \boldsymbol{u}_\mathrm{s} \tag{1b}$$

where $\omega_\mathrm{r} = \omega_\mathrm{s} - \omega_\mathrm{m}$ is the slip angular frequency, $\boldsymbol{u}_\mathrm{s}$ is the stator voltage, $\alpha = R_\mathrm{R}/L_\mathrm{M}$ is the inverse rotor time constant, and $\beta = R_\mathrm{s}/L_\sigma + \omega_\mathrm{rb}$, where $\omega_\mathrm{rb} = (1/L_\mathrm{M} + 1/L_\sigma)R_\mathrm{R}$ is

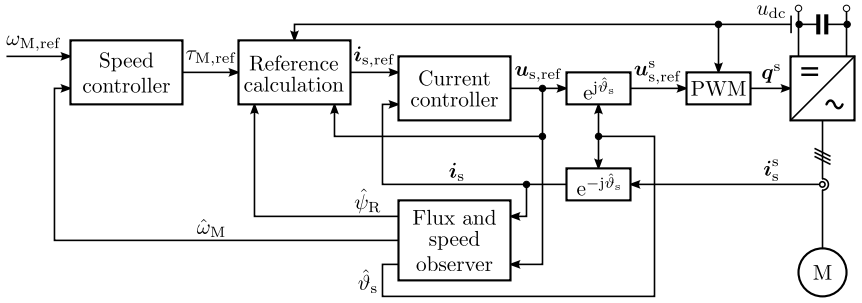

Fig. 2. Speed-sensorless vector controlled induction motor drive.

the breakdown slip frequency. The rotor flux linkage and the electromagnetic torque, respectively, are given by

$$\boldsymbol{\psi}_{\mathrm{R}} = \boldsymbol{\psi}_{\mathrm{s}} - L_\sigma \boldsymbol{i}_{\mathrm{s}} \tag{1c}$$

$$\tau_{\mathrm{m}} = \boldsymbol{i}_{\mathrm{s}}^{\mathrm{T}} \mathbf{J} \boldsymbol{\psi}_{\mathrm{s}} \tag{1d}$$

where per-unit (p.u.) quantities are assumed in the torque equation.

III. Flux Observers

The reduced-order observer is briefly presented for comparison, followed by a description of the proposed full-order observer design. Fig. 2 shows a block diagram of a general sensorless vector controlled induction motor drive, in which the flux observer is either the reduced or the full-order observer.

A. Reduced-Order Observer

If good-quality measurement of the stator current $\boldsymbol{i}_{\mathrm{s}}$ is available, a reduced-order flux observer can be applied [10]. Using (1a), the reduced-order observer can be formulated as [1]

$$\frac{\mathrm{d}\hat{\boldsymbol{\psi}}_{\mathrm{s}}}{\mathrm{d}t} = -\omega_{\mathrm{s}} \mathbf{J} \hat{\boldsymbol{\psi}}_{\mathrm{s}} - R_{\mathrm{s}} \boldsymbol{i}_{\mathrm{s}} + \boldsymbol{u}_{\mathrm{s}} + \boldsymbol{K} \boldsymbol{e} \tag{2a}$$

$$\hat{\boldsymbol{\psi}}_{\mathrm{R}} = \hat{\boldsymbol{\psi}}_{\mathrm{s}} - L_\sigma \boldsymbol{i}_{\mathrm{s}} \tag{2b}$$

where $\boldsymbol{K}$ is a 2×2 observer gain matrix. The correction vector is obtained from (1b),

$$\boldsymbol{e} = L_\sigma \frac{\mathrm{d}\boldsymbol{i}_{\mathrm{s}}}{\mathrm{d}t} + L_\sigma \left(\beta \mathbf{I} + \hat{\omega}_{\mathrm{r}} \mathbf{J}\right) \boldsymbol{i}_{\mathrm{s}} - (\alpha \mathbf{I} - \hat{\omega}_{\mathrm{m}} \mathbf{J}) \hat{\boldsymbol{\psi}}_{\mathrm{s}} - \boldsymbol{u}_{\mathrm{s}} \tag{2c}$$

where $\hat{\omega}_{\mathrm{m}}$ is the speed estimate and $\hat{\omega}_{\mathrm{r}} = \omega_{\mathrm{s}} - \hat{\omega}_{\mathrm{m}}$ is the slip estimate. The speed is estimated by integrating the component of the correction vector $\boldsymbol{e}$ orthogonal to the rotor flux estimate, i.e., [11]

$$\frac{\mathrm{d}\hat{\omega}_{\mathrm{m}}}{\mathrm{d}t} = \boldsymbol{k}_\omega^{\mathrm{T}} \boldsymbol{e} \tag{3a}$$

where the gain vector is

$$\boldsymbol{k}_\omega^{\mathrm{T}} = \alpha_{\mathrm{o}} \frac{\hat{\boldsymbol{\psi}}_{\mathrm{R}}^{\mathrm{T}} \mathbf{J}}{\|\hat{\boldsymbol{\psi}}_{\mathrm{R}}\|^2} \tag{3b}$$

and α_{o} is the speed-estimation bandwidth.[1]

As special cases, $\boldsymbol{K} = \mathbf{0}$ yields the voltage model and $\boldsymbol{K} = \mathbf{I}$ yields the current model. A general inherently sensorless stabilizing gain, allowing arbitrary pole placement for the linearized estimation-error dynamics, is available [1]. Here, its special case is used

$$\boldsymbol{K} = \frac{b(\alpha \mathbf{I} + \hat{\omega}_{\mathrm{m}} \mathbf{J})}{\alpha^2 + \hat{\omega}_{\mathrm{m}}^2} \frac{\hat{\boldsymbol{\psi}}_{\mathrm{R}} \hat{\boldsymbol{\psi}}_{\mathrm{R}}^{\mathrm{T}}}{\|\hat{\boldsymbol{\psi}}_{\mathrm{R}}\|^2} \tag{4}$$

where the positive design parameter b defines the decay rate of the estimation error.

It is be noted that the time derivative of the stator current in (2c) is integrated both in (2a) and (3a), and, therefore, no derivative terms remain in the state estimates. Furthermore, the terms containing estimated speed or slip in the correction vector $\boldsymbol{e}$ cancel out with the observer gain matrix (4). This can be verified, e.g., by substituting the rotor flux estimate from (2b) in (2c), i.e.

$$\boldsymbol{e} = L_\sigma \frac{\mathrm{d}\boldsymbol{i}_{\mathrm{s}}}{\mathrm{d}t} - (\alpha \mathbf{I} - \hat{\omega}_{\mathrm{m}} \mathbf{J}) \hat{\boldsymbol{\psi}}_{\mathrm{R}} + [(R_{\mathrm{s}} + R_{\mathrm{R}}) \mathbf{I} + \omega_{\mathrm{s}} L_\sigma \mathbf{J}] \boldsymbol{i}_{\mathrm{s}} - \boldsymbol{u}_{\mathrm{s}} \tag{5}$$

and since $\boldsymbol{K} \mathbf{J} \hat{\boldsymbol{\psi}}_{\mathrm{R}} = \mathbf{0}_{2,1}$ the speed estimate $\hat{\omega}_{\mathrm{m}}$ is cancels out in (2a).

B. Full-Order Observer

Next, the full-order flux observer is considered,

$$\frac{\mathrm{d}\hat{\boldsymbol{\psi}}_{\mathrm{s}}}{\mathrm{d}t} = -\omega_{\mathrm{s}} \mathbf{J} \hat{\boldsymbol{\psi}}_{\mathrm{s}} - R_{\mathrm{s}} \hat{\boldsymbol{i}}_{\mathrm{s}} + \boldsymbol{u}_{\mathrm{s}} + \boldsymbol{K}_\psi \tilde{\boldsymbol{i}}_{\mathrm{s}} \tag{6a}$$

$$L_\sigma \frac{\mathrm{d}\hat{\boldsymbol{i}}_{\mathrm{s}}}{\mathrm{d}t} = (\alpha \mathbf{I} - \hat{\omega}_{\mathrm{m}} \mathbf{J}) \hat{\boldsymbol{\psi}}_{\mathrm{s}} - L_\sigma \left(\beta \mathbf{I} + \hat{\omega}_{\mathrm{r}} \mathbf{J}\right) \hat{\boldsymbol{i}}_{\mathrm{s}} + \boldsymbol{u}_{\mathrm{s}} + \boldsymbol{K}_{\mathrm{i}} \tilde{\boldsymbol{i}}_{\mathrm{s}} \tag{6b}$$

$$\hat{\boldsymbol{\psi}}_{\mathrm{R}} = \hat{\boldsymbol{\psi}}_{\mathrm{s}} - L_\sigma \hat{\boldsymbol{i}}_{\mathrm{s}} \tag{6c}$$

where $\tilde{\boldsymbol{i}}_{\mathrm{s}} = \boldsymbol{i}_{\mathrm{s}} - \hat{\boldsymbol{i}}_{\mathrm{s}}$ is the estimation error of the stator current. The proposed observer gains $\boldsymbol{K}_\psi$ and $\boldsymbol{K}_{\mathrm{i}}$ are defined as

$$\boldsymbol{K}_\psi = \alpha_{\mathrm{i}} L_\sigma \boldsymbol{K} - R_{\mathrm{s}} \mathbf{I} \tag{6d}$$

$$\boldsymbol{K}_{\mathrm{i}} = L_\sigma [(\alpha_{\mathrm{i}} - \beta) \mathbf{I} - \hat{\omega}_{\mathrm{r}} \mathbf{J}] \tag{6e}$$

[1] In estimated rotor-flux coordinates, the speed estimator in (3a) is equivalently expressed as $\mathrm{d}\hat{\omega}_{\mathrm{m}}/\mathrm{d}t = \alpha_{\mathrm{o}} \left(\omega_{\mathrm{s}} - R_{\mathrm{R}} i_{\mathrm{sq}} / \hat{\psi}_{\mathrm{R}} - \hat{\omega}_{\mathrm{m}}\right)$, where i_{sq} is the imaginary component of the stator current in the estimated rotor-flux coordinates, and $\hat{\psi}_{\mathrm{R}}$ is the magnitude of the rotor flux [1].

where $\boldsymbol{K}$ is the observer gain matrix defined in (4) and α_i is a positive parameter defining decay rate of the stator current estimation error. These gains together make it possible to decouple the flux-estimation error dynamics from the speed estimate, as will be shown later.

The speed is estimated using a proportional-integral (PI) -type adaptation law as

$$\frac{\mathrm{d}\hat{\omega}_\mathrm{m}}{\mathrm{d}t} = L_\sigma \boldsymbol{k}_\omega^\mathrm{T} \left(\frac{\mathrm{d}\tilde{\boldsymbol{i}}_\mathrm{s}}{\mathrm{d}t} + \alpha_\mathrm{i} \tilde{\boldsymbol{i}}_\mathrm{s} \right) \tag{6f}$$

where $\boldsymbol{k}_\omega^\mathrm{T}$ is the gain vector defined in (3b).

IV. Analysis

The estimation error dynamics of the two observers are analyzed by means of small-signal linearization. The small-signal deviation of the stator current about an operating point is denoted by $\Delta\boldsymbol{i}_\mathrm{s} = \boldsymbol{i}_\mathrm{s} - \boldsymbol{i}_\mathrm{s0}$, where $\boldsymbol{i}_\mathrm{s0}$ is the operating-point current. Other small-signal and operating-point quantities are marked similarly. For simplicity, the inverter is assumed ideal and the parameter errors are omitted.

A. Reduced-Order Observer

The motor model (1) and the observer (2) are linearized, leading to [1]

$$\begin{aligned}\frac{\mathrm{d}\Delta\tilde{\boldsymbol{\psi}}_\mathrm{s}}{\mathrm{d}t} &= -\left[\omega_\mathrm{s0}\mathbf{J} + \boldsymbol{K}_0\left(\alpha\mathbf{I} - \omega_\mathrm{m0}\mathbf{J}\right)\right]\Delta\tilde{\boldsymbol{\psi}}_\mathrm{s} \\ &\quad + \boldsymbol{K}_0\mathbf{J}\boldsymbol{\psi}_\mathrm{R0}\Delta\tilde{\omega}_\mathrm{m} \end{aligned} \tag{7a}$$

$$\frac{\mathrm{d}\Delta\hat{\omega}_\mathrm{m}}{\mathrm{d}t} = \boldsymbol{k}_{\omega0}^\mathrm{T}\left(\alpha\mathbf{I} - \omega_\mathrm{m0}\mathbf{J}\right)\Delta\tilde{\boldsymbol{\psi}}_\mathrm{s} + \alpha_\mathrm{o}\Delta\tilde{\omega}_\mathrm{m} \tag{7b}$$

where $\Delta\tilde{\omega}_\mathrm{m} = \Delta\omega_\mathrm{m} - \Delta\hat{\omega}_\mathrm{m}$. The operating point observer gain $\boldsymbol{K}_0$ and the gain vector $\boldsymbol{k}_{\omega0}^\mathrm{T}$ are, respectively,

$$\boldsymbol{K}_0 = \frac{b(\alpha\mathbf{I} + \omega_\mathrm{m0}\mathbf{J})}{\alpha^2 + \omega_\mathrm{m0}^2}\frac{\boldsymbol{\psi}_\mathrm{R0}\boldsymbol{\psi}_\mathrm{R0}^\mathrm{T}}{\|\boldsymbol{\psi}_\mathrm{R0}\|^2} \tag{8a}$$

$$\boldsymbol{k}_{\omega0}^\mathrm{T} = \alpha_\mathrm{o}\frac{\boldsymbol{\psi}_\mathrm{R0}^\mathrm{T}\mathbf{J}}{||\boldsymbol{\psi}_\mathrm{R0}||^2} \tag{8b}$$

Since $\boldsymbol{K}_0\mathbf{J}\boldsymbol{\psi}_\mathrm{R0} = \mathbf{0}_{2,1}$ holds for the observer gain, the flux and torque estimation dynamics are decoupled from the speed estimate as well as from the speed input. The speed estimate $\hat{\omega}_\mathrm{m}$ appearing in the observer gain (4) introduces no coupling in the linearized model since the operating-point estimation errors are zero under the assumption of accurate parameter estimates.

From (7b), the linearized speed-estimation dynamics in the Laplace domain are

$$\frac{\Delta\hat{\omega}_\mathrm{m}(s)}{\Delta\omega_\mathrm{m}(s)} = \frac{\alpha_\mathrm{o}}{s + \alpha_\mathrm{o}} \tag{9}$$

Furthermore, the observer characteristic polynomial is

$$D_\mathrm{ro}(s) = (s^2 + bs + \omega_\mathrm{s0}^2)(s + \alpha_\mathrm{o}) \tag{10}$$

The parameter b in (4) is recommended to be scheduled as [12]

$$b = 2\zeta_\infty|\omega_\mathrm{s}| + \alpha \tag{11}$$

where ζ_∞ is the desired damping ratio at high speeds. Due to the additional term α in (11), the flux estimation poles placed at $s = 0$ and $s = -\alpha$ at zero stator frequency $\omega_\mathrm{s} = 0$. Placing both poles at $s = 0$ would result in an unstable system and unnecessary complications for the magnetization and starting of the motor.

B. Full-Order Observer

The estimation-error dynamics are obtained by applying (1) and (6), which after linearization become

$$\frac{\mathrm{d}\Delta\tilde{\boldsymbol{\psi}}_\mathrm{s}}{\mathrm{d}t} = -\omega_\mathrm{s0}\mathbf{J}\Delta\tilde{\boldsymbol{\psi}}_\mathrm{s} - \alpha_\mathrm{i}L_\sigma\boldsymbol{K}_0\Delta\tilde{\boldsymbol{i}}_\mathrm{s} \tag{12a}$$

$$L_\sigma\frac{\mathrm{d}\Delta\tilde{\boldsymbol{i}}_\mathrm{s}}{\mathrm{d}t} = (\alpha\mathbf{I} - \omega_\mathrm{m0}\mathbf{J})\Delta\tilde{\boldsymbol{\psi}}_\mathrm{s} - \alpha_\mathrm{i}L_\sigma\Delta\tilde{\boldsymbol{i}}_\mathrm{s} - \mathbf{J}\boldsymbol{\psi}_\mathrm{R0}\Delta\tilde{\omega}_\mathrm{m} \tag{12b}$$

$$\frac{\mathrm{d}\Delta\hat{\omega}_\mathrm{m}}{\mathrm{d}t} = L_\sigma\boldsymbol{k}_{\omega0}^\mathrm{T}\left(\frac{\mathrm{d}\Delta\tilde{\boldsymbol{i}}_\mathrm{s}}{\mathrm{d}t} + \alpha_\mathrm{i}\Delta\tilde{\boldsymbol{i}}_\mathrm{s}\right) \tag{12c}$$

From (12), the linearized stator flux and current estimation error dynamics in the Laplace domain are

$$\Delta\tilde{\boldsymbol{\psi}}_\mathrm{s}(s) = -(s\mathbf{I} + \omega_\mathrm{s0}\mathbf{J})^{-1}\alpha_\mathrm{i}L_\sigma\boldsymbol{K}_0\Delta\tilde{\boldsymbol{i}}_\mathrm{s}(s) \tag{13a}$$

$$\Delta\tilde{\boldsymbol{i}}_\mathrm{s}(s) = \frac{(\alpha\mathbf{I} - \omega_\mathrm{m0}\mathbf{J})\Delta\tilde{\boldsymbol{\psi}}_\mathrm{s}(s) - \mathbf{J}\boldsymbol{\psi}_\mathrm{R0}\Delta\tilde{\omega}_\mathrm{m}(s)}{L_\sigma(s + \alpha_\mathrm{i})} \tag{13b}$$

Substituting (13b) in (13a) reveals that the flux estimation-error dynamics are decoupled from the speed-estimate since $\boldsymbol{K}_0\mathbf{J}\boldsymbol{\psi}_\mathrm{R0} = \mathbf{0}_{2,1}$.

Furthermore, by substituting (12b) in (12c), the linearized speed-estimation dynamics become equivalent to the reduced-order observer in (7b) and (9), i.e.

$$\frac{\Delta\hat{\omega}_\mathrm{m}(s)}{\Delta\omega_\mathrm{m}(s)} = \frac{\alpha_\mathrm{o}}{s + \alpha_\mathrm{o}} \tag{14}$$

If a speed estimate is needed, e.g., for speed control, the integral state of the PI adaptation law in (6f) may be used. The dynamics of the integral state $\hat{\omega}_\mathrm{mi}$ are governed by

$$\frac{\Delta\hat{\omega}_\mathrm{mi}(s)}{\Delta\omega_\mathrm{m}(s)} = \frac{\alpha_\mathrm{o}}{s + \alpha_\mathrm{o}}\frac{\alpha_\mathrm{i}}{s + \alpha_\mathrm{i}} \tag{15}$$

From (12), the observer characteristic polynomial is computed

$$D_\mathrm{fo}(s) = \left(s^2 + bs\frac{\alpha_\mathrm{i}}{s + \alpha_\mathrm{i}} + \omega_\mathrm{s0}^2\right)(s + \alpha_\mathrm{i})^2(s + \alpha_\mathrm{o}) \tag{16}$$

These poles are stable for positive design parameters b, α_i, and α_o. With $\alpha_\mathrm{i} = 0$ the flux-estimation poles correspond to the pure voltage model, while α_i approaching infinity tends the poles towards the poles of the reduced-order observer in (10).

V. Results

The two observer designs are studied by means of experiments. A 2.2-kW 50-Hz 400-V four-pole induction motor is selected as an example motor. Table I gives the parameters and rated values of the motor. Fig. 2 shows the block diagram of the used speed-sensorless vector control algorithm, where conventional PI controllers are used for the speed and current

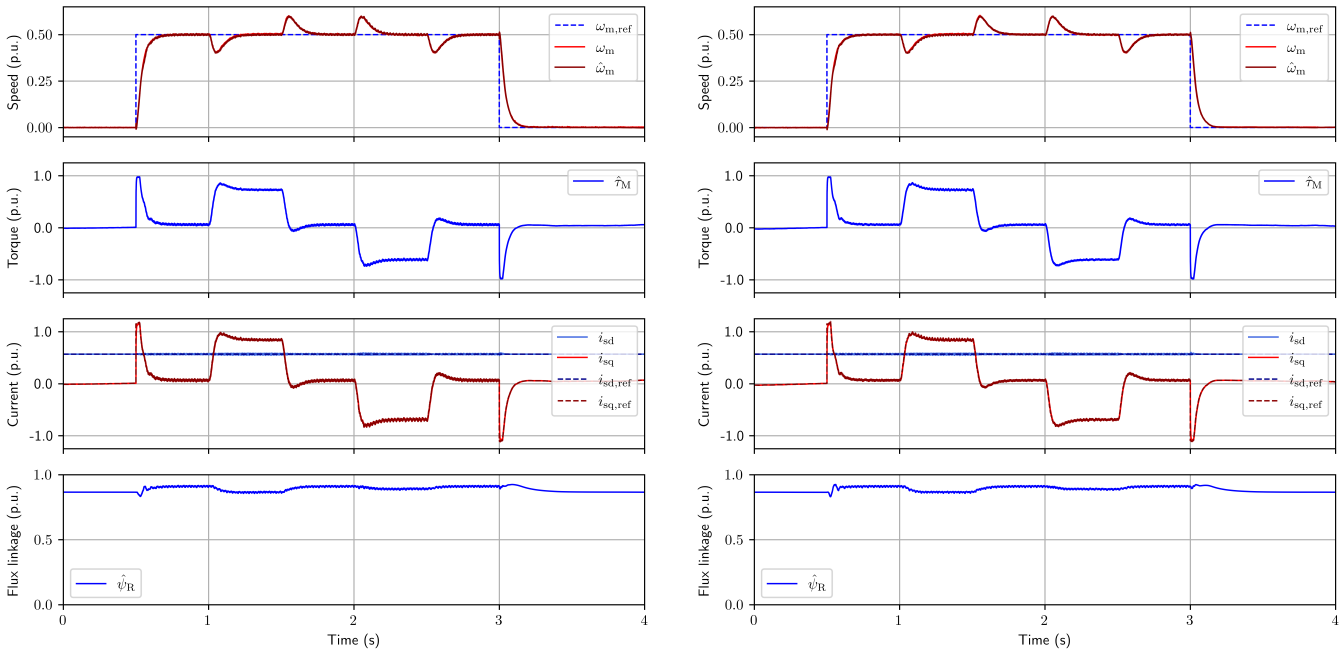

(a) (b)

Fig. 3. Experimental result: Middle-speed operation for (a) reduced-order observer and (b) full-order observer. The speed reference is changed stepwise: $0 \rightarrow 0.5$ p.u. $\rightarrow 0$. Rated load torque (0.66 p.u.) in the positive and negative direction is applied stepwise at $t = 1$ s and $t = 2$ s, respectively.

TABLE I
DATA OF THE 2.2-KW FOUR-POLE INDUCTION MOTOR

Rated values		
Voltage (line-to-neutral, peak value)	$\sqrt{2/3}$·400 V	1 p.u.
Current (peak value)	$\sqrt{2}$·5 A	1 p.u.
Frequency	50 Hz	1 p.u.
Speed	1 430 r/min	0.95 p.u.
Torque	14.6 Nm	0.66 p.u.
Parameters		
Stator resistance R_s	3.7 Ω	0.080 p.u.
Rotor resistance R_R	2.1 Ω	0.045 p.u.
Leakage inductance L_σ	21 mH	0.143 p.u.
Magnetizing inductance L_M	224 mH	1.524 p.u.
Total inertia J_m	0.0155 kgm^2	67.1 p.u.

control. The reference calculation algorithm includes a field-weakening method, which is based on [13].

The control algorithms were implemented on a dSPACE MicroLabBox prototyping unit. For monitoring purposes, the rotor speed was measured using a resolver. Sampling was synchronized to the PWM, and double sampling was used. The switching frequency was set to 4 kHz. Constant motor parameters were used and saturation of the inductances was not considered. The inverter nonlinearities were compensated for with a current feedforward method [14]. Furthermore, both observers were implemented in the estimated rotor flux coordinates, as detailed in Appendix A.

In both cases, the bandwidth of the speed controller is $\alpha_s = 2\pi \cdot 4$ rad/s and the bandwidth of the current controller is $\alpha_c = 2\pi \cdot 150$ rad/s. For the observer parameters, a speed-estimation bandwidth $\alpha_o = 2\pi \cdot 40$ rad/s is used, and the estimation decay rate parameter is scheduled as $b = 2\zeta_\infty |\omega_{m0}| + \alpha$, where the desired damping ratio at high speeds is selected as $\zeta_\infty = 0.2$ [12]. For the full-order observer the integral state $\hat{\omega}_{mi}$ of the speed speed estimate used in the speed controller. Furthermore, $\alpha_i = 2\pi \cdot 600$ rad/s is used.

Fig. 3 shows an experimental result in the medium speed region for the reduced-order observer and the full-order order observer with the proposed gain selection. The speed reference is stepped from zero to 0.5 p.u. at $t = 0.5$ s. The rated load torque is applied stepwise at $t = 1$ s and $t = 2$ s in the positive and negative directions, respectively. As expected based on the analysis, the results do not show significant difference between the two observers.

Fig. 4 shows an experimental result of operation in the field-weakening region. The speed reference is stepped to 2 p.u. at $t = 0.5$ s. No load torque is applied. The observers function very similarly, but a small difference can be noticed during the fast transient around $t = 0.75$ s, as could be expected based on the analysis.

Fig. 5 shows an experimental result of low-speed reversals under rated load torque. This is a challenging test sequence for speed-sensorless control since all operating modes, i.e. motoring, plugging and regenerating, are visited. Sustained operation at zero stator frequency under load torque is a fundamental limitation for sensorless induction motor drives [15]. The duration that the drive can remain in this operating point without losing stability depends not only on the design of the observer but also on the accuracy of the parameter estimates and the compensation of the inverter nonlinearities.

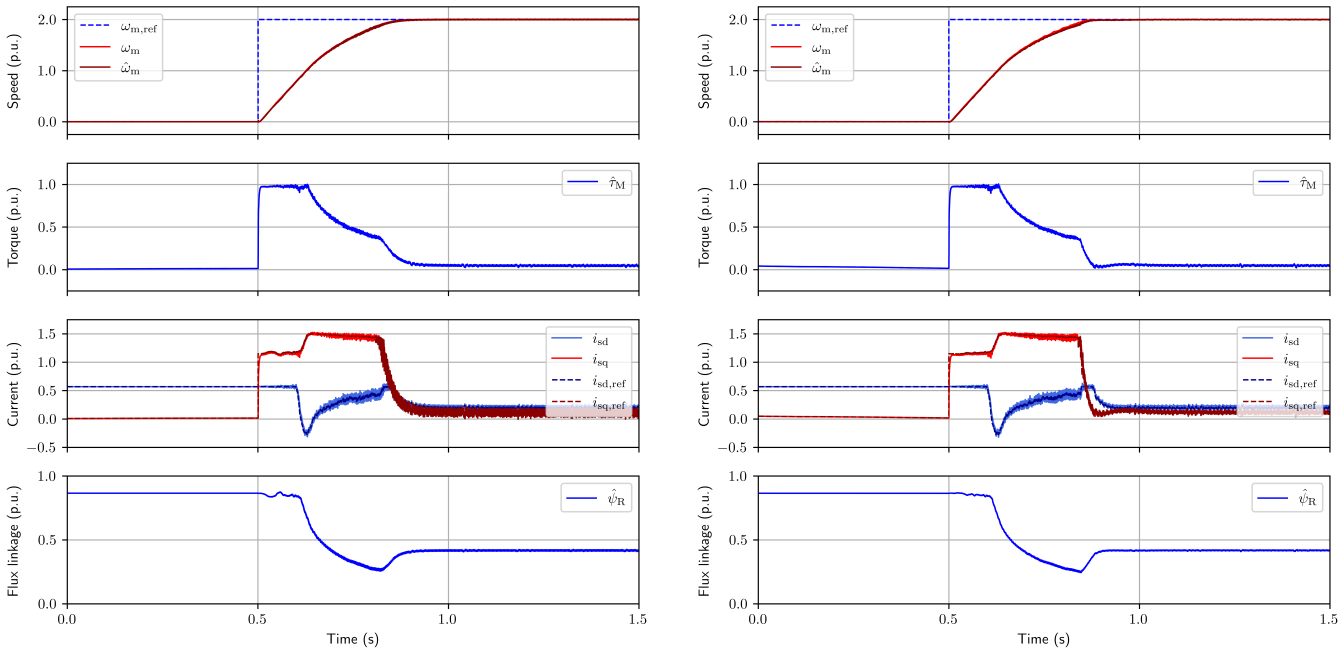

(a) (b)

Fig. 4. Experimental result: High-speed operation for (a) reduced-order observer (b) full-order observer. The speed reference is increased stepwise: $0 \rightarrow 2$ p.u. No load torque is applied.

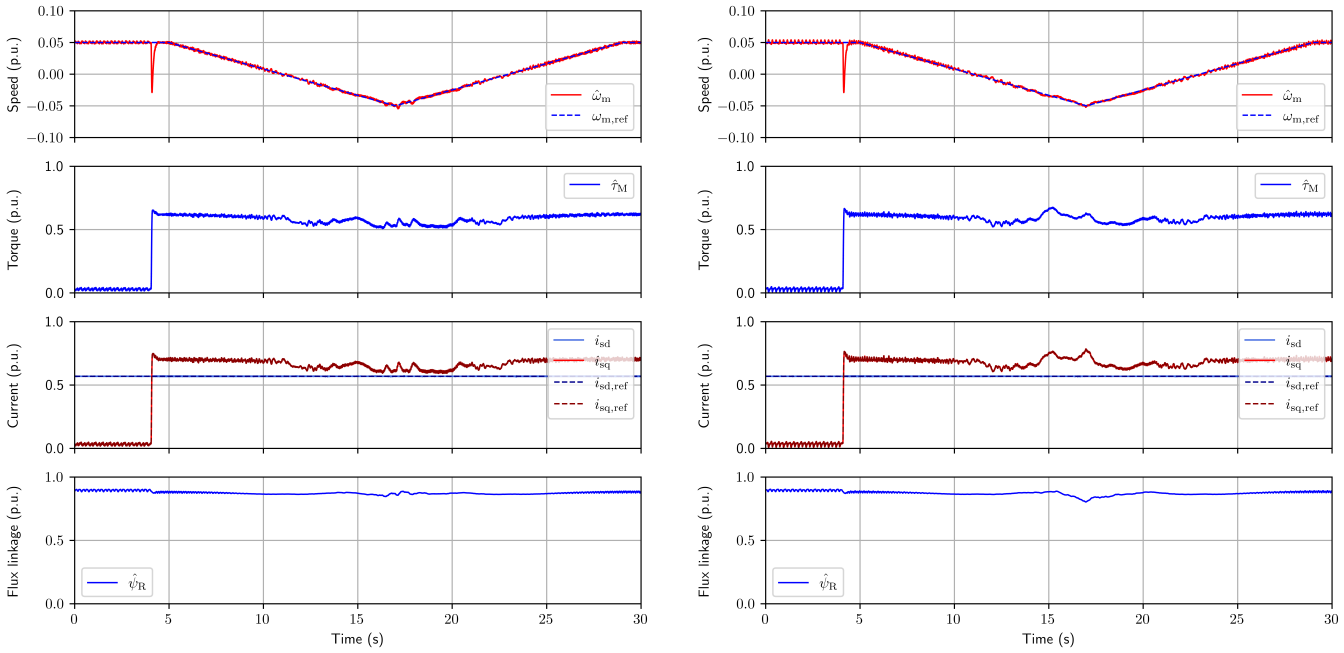

(a) (b)

Fig. 5. Experimental result: Low-speed reversals under rated load torque for (a) reduced-order observer (b) full-order observer.

Performance could be improved with, e.g., stator resistance adaptation and accounting for the saturation of the inductances [1], [7].

VI. Conclusion

This paper revisited the full-order observer for induction motor. A new observer design is proposed, which decouples the flux estimation dynamics from the speed estimate. A closed-form analytical expression for the complete full-order observer estimation-error dynamics is derived, including the effect of the speed-adaptation.

References

[1] M. Hinkkanen, L. Harnefors, and J. Luomi, "Reduced-order flux observers with stator-resistance adaptation for speed-sensorless induction motor drives," *IEEE Trans. Power Electron.*, vol. 25, no. 5, pp. 1173–1183, May 2010.

[2] H. Kubota, K. Matsuse, and T. Nakano, "DSP-based speed adaptive flux observer of induction motor," *IEEE Trans. Ind. Appl.*, vol. 29, no. 2, pp. 344–348, Mar./Apr. 1993.

[3] G. Yang and T.-H. Chin, "Adaptive-speed identification scheme for a vector-controlled speed sensorless inverter-induction motor drive," *IEEE Trans. Ind. Appl.*, vol. 29, no. 4, pp. 820–825, Jul./Aug. 1993.

[4] M. Hinkkanen and J. Luomi, "Stabilization of regenerating-mode operation in sensorless induction motor drives by full-order flux observer design," *IEEE Trans. Ind. Electron.*, vol. 51, no. 6, pp. 1318–1328, Dec. 2004.

[5] L. Harnefors, "Globally stable speed-adaptive observers for sensorless induction motor drives," *IEEE Trans. Ind. Electron.*, vol. 54, no. 2, pp. 1243–1245, Apr. 2007.

[6] S. Sangwongwanich, S. Suwankawin, S. Po-ngam, and S. Koonlaboon, "A unified speed estimation design framework for sensorless ac motor drives based on positive-real property," in *Proc. PCC-Nagoya*, Nagoya, Japan, Apr. 2007, pp. 1111–1118.

[7] Z. Qu, M. Hinkkanen, and L. Harnefors, "Gain scheduling of a full-order observer for sensorless induction motor drives," *IEEE Trans. Ind. Appl.*, vol. 50, no. 6, pp. 3834–3845, Nov./Dec. 2014.

[8] G. R. Slemon, "Modelling of induction machines for electric drives," *IEEE Trans. Ind. Appl.*, vol. 25, no. 6, pp. 1126–1131, Nov./Dec. 1989.

[9] J. Holtz, "The representation of ac machine dynamics by complex signal flow graphs," *IEEE Trans. Ind. Electron.*, vol. 42, no. 3, pp. 263–271, Jun. 1995.

[10] G. C. Verghese and S. R. Sanders, "Observers for flux estimation in induction machines," *IEEE Trans. Ind. Electron.*, vol. 35, no. 1, pp. 85–94, Feb. 1988.

[11] L. Harnefors and M. Hinkkanen, "Complete stability of reduced-order and full-order observers for sensorless IM drives," *IEEE Trans. Ind. Electron.*, vol. 55, no. 3, pp. 1319–1329, Mar. 2008.

[12] L. Tiitinen, M. Hinkkanen, and L. Harnefors, "Stable and passive observer-based V/Hz control for induction motors," in *Proc. IEEE ECCE*, Detroit, MI, Oct. 2022.

[13] M. Hinkkanen and J. Luomi, "Braking scheme for vector-controlled induction motor drives equipped with diode rectifier without braking resistor," *IEEE Trans. Ind. Appl.*, vol. 42, no. 5, pp. 1257–1263, Sep./Oct. 2006.

[14] J.-W. Choi and S.-K. Sul, "Inverter output voltage synthesis using novel dead time compensation," *IEEE Trans. Power Electron.*, vol. 11, no. 2, pp. 221–227, Mar. 1996.

[15] J. Holtz and J. Quan, "Sensorless vector control of induction motors at very low speed using a nonlinear inverter model and parameter identification," *IEEE Trans. Ind. Appl.*, vol. 38, no. 4, pp. 1087–1095, Jul./Aug. 2002.

Appendix A
Implementation in Estimated Rotor-Flux Coordinates

If the rotor flux linkage is needed in sensorless control, implementation of the observer may be more natural by selecting the rotor flux and the stator current as the state variables. With this selection, the full-order observer becomes

$$L_\sigma \frac{\mathrm{d}\hat{\boldsymbol{i}}_\mathrm{s}}{\mathrm{d}t} = -(R_\sigma \mathbf{I} + \omega_\mathrm{s} L_\sigma \mathbf{J})\hat{\boldsymbol{i}}_\mathrm{s} + (\alpha \mathbf{I} - \hat{\omega}_\mathrm{m}\mathbf{J})\hat{\boldsymbol{\psi}}_\mathrm{R} + \boldsymbol{u}_\mathrm{s} + \boldsymbol{K}'_\mathrm{i}\tilde{\boldsymbol{i}}_\mathrm{s} \tag{17a}$$

$$\frac{\mathrm{d}\hat{\boldsymbol{\psi}}_\mathrm{R}}{\mathrm{d}t} = R_\mathrm{R}\hat{\boldsymbol{i}}_\mathrm{s} - (\alpha \mathbf{I} + \hat{\omega}_\mathrm{r}\mathbf{J})\hat{\boldsymbol{\psi}}_\mathrm{R} + \boldsymbol{K}'_\psi \tilde{\boldsymbol{i}}_\mathrm{s} \tag{17b}$$

The following observer gains result in the identical observer dynamics as (6) with the proposed observer gains in (6d):

$$\boldsymbol{K}'_\psi = \alpha_\mathrm{i} L_\sigma \boldsymbol{K} - \boldsymbol{K}_\mathrm{i} - R_\mathrm{s}\mathbf{I} \tag{18a}$$

$$\boldsymbol{K}'_\mathrm{i} = L_\sigma(\gamma \mathbf{I} - \hat{\omega}_\mathrm{r}\mathbf{J}) - R_\sigma \mathbf{I} \tag{18b}$$

where $\gamma = \alpha_\mathrm{i} - \alpha$.

In estimated rotor flux coordinates $\hat{\boldsymbol{\psi}}_\mathrm{R} = [\hat{\psi}_\mathrm{R}, 0]^\mathrm{T}$ holds. Therefore, the observer in (17) can be written in component form as

$$L_\sigma \frac{\mathrm{d}\hat{i}_\mathrm{sd}}{\mathrm{d}t} = \alpha\hat{\psi}_\mathrm{R} - R_\sigma i_\mathrm{sd} + \omega_\mathrm{s} L_\sigma i_\mathrm{sq} + u_\mathrm{sd} + L_\sigma(\gamma\tilde{i}_\mathrm{sd} - \hat{\omega}_\mathrm{m}\tilde{i}_\mathrm{sq}) \tag{19a}$$

$$L_\sigma \frac{\mathrm{d}\hat{i}_\mathrm{sq}}{\mathrm{d}t} = -\hat{\omega}_\mathrm{m}\hat{\psi}_\mathrm{R} - R_\sigma i_\mathrm{sq} - \omega_\mathrm{s} L_\sigma i_\mathrm{sd} + u_\mathrm{sq} + L_\sigma(\gamma\tilde{i}_\mathrm{sq} + \hat{\omega}_\mathrm{m}\tilde{i}_\mathrm{sd}) \tag{19b}$$

$$\frac{\mathrm{d}\hat{\psi}_\mathrm{R}}{\mathrm{d}t} = -\alpha\hat{\psi}_\mathrm{R} + R_\mathrm{R} i_\mathrm{sd} + (k_1\alpha_\mathrm{i} - \gamma)L_\sigma\tilde{i}_\mathrm{sd} - (\omega_\mathrm{s} - \hat{\omega}_\mathrm{m})L_\sigma\tilde{i}_\mathrm{sq} \tag{19c}$$

$$\omega_\mathrm{s} = \hat{\omega}_\mathrm{m} + \frac{R_\mathrm{R} i_\mathrm{sq} + k_2\alpha_\mathrm{i} L_\sigma\tilde{i}_\mathrm{sd} - \gamma L_\sigma\tilde{i}_\mathrm{sq}}{\hat{\psi}_\mathrm{R} - L_\sigma\tilde{i}_\mathrm{sd}} \tag{19d}$$

where $k_1 = b\alpha/(\alpha^2 + \hat{\omega}_\mathrm{m}^2)$ and $k_2 = b\hat{\omega}_\mathrm{m}/(\alpha^2 + \hat{\omega}_\mathrm{m}^2)$. Implementation in the estimated rotor-flux coordinates for the reduced-order observer is shown in [1].